EJMO

DOI: 10.14744/ejmo.2023.29445
EJMO 2023;7(2):143–159

Research Article

Comprehensive Analysis of Biologic and Prognostic Implication for ZNF536 in Pan-Cancer

Yuan Fang,[1,2] Shu-jing Wang,[3] Qiang Wu[1]

[1]Department of Pathology, The Second Hospital of Anhui Medical University, Hefei, China
[2]Department of Pathology, Anhui Provincial Children's Hospital, Hefei, China
[3]School of Basic Medical Sciences, Anhui Medical University, Hefei, China

Abstract

Objectives: Zinc Finger Protein 536 (ZNF536) is a highly conserved zinc finger protein, acting as DNA-binding transcription suppressor, and negatively regulating neuron differentiation. However, the role of ZNF536 in cancers is still unknown.

Methods: In this study, we aim to comprehensively explore the biologic and prognostic implication of ZNF536 in pan-cancer by multi-layered analysis. The mRNA differential expression and DNA methylation of ZNF536 in pan-cancer and normal controls based on The Cancer Genome Atlas (TCGA) and Genotype Tissue-Expression (GTEx) data were interpreted. Immunohistochemistry was performed on a tissue micro-array to detect the protein expression of ZNF536. The prognostic implication of ZNF536 in pan-cancer was studied by survival analysis. The cBioPortal database was used to display ZNF536 genomic alterations. The co-expression of ZNF536 and immune-related genes in pan-cancer was investigated. Further research was made on the relationship between ZNF536 expression and tumor immune microenvironment. CancerSEA was employed to excavate the ZNF536 expression at single cell level with different cancer function. The biological function of ZNF536 in pan-cancer was exhibited by gene enrichment analysis.

Results: The ZNF536 mRNA was highly expressed in 4 out of 33 cancers, but lowly expressed in 22 cancers. Immunohistochemistry on the tissue micro-array confirmed the high expression of ZNF536 protein in pancreatic adenocarcinoma (PAAD) and low expression in stomach adenocarcinoma (STAD). DNA hypermethylation in prostate adenocarcinoma (PRAD) was observed, which might result in its down-regulated expression. High expression of ZNF536 predicted poor prognosis in 5 cancers, but predicted favorable prognosis in 2 cancers. Genomic alterations of ZNF536 showed mutation in 26 cancers and amplification in 20 cancers. The altered group usually had worse prognosis. ZNF536 mRNA expression was correlated with the degree of immune infiltrates in pan-cancer. Single cell sequencing and gene enrichment analysis showed that the ZNF536-correlated genes might regulate a variety of biological processes in pan-cancer, mainly via angiogenesis pathway.

Conclusion: Our results indicated that ZNF536 might be a prognostic and immune-related biomarker for specific malignancies through the angiogenesis pathway.

Keywords: Immune, pan-cancer, prognosis, tissue micro-array, ZNF536

Cite This Article: *Fang Y, Wang S, Wu Q. Comprehensive Analysis of Biologic and Prognostic Implication for ZNF536 in Pan-Cancer. EJMO 2023;7(2):143–159.*

Zinc finger proteins constitute one of the biggest families of transcription factors in human genetics, characterized by conserved zinc finger motifs. They are essential for several biological processes, including apoptosis, differentiation and development.[1] Moreover, recent researches have demonstrated that zinc finger proteins participated in the development in multiple cancers. In colon adenocarcinoma, zinc finger protein 750 (ZNF750) facilitated car-

Address for correspondence: Qiang Wu, MD. Anhui Medical University, 81 Meishan Road, Hefei, China
Phone: 0551-65161025 **E-mail:** wuqiang@ahmu.edu.cn

Submitted Date: March 28, 2023 **Accepted Date:** May 08, 2023 **Available Online Date:** June 19, 2023

cinogenesis and influenced pharmacotherapy response, the former function exerted through up-regulating the long non-coding RNA CYTOR.[2] Another two zinc finger proteins, ZNF384 and ZNF655, promoted tumor progression via transcriptional regulation of Cyclin D1 and AURKA in hepatocellular carcinoma and glioma, respectively.[3,4] In addition, a zinc finger gene signature, covering ZNF644, ZNF341, ZNF541 and ZNF653, was identified as a predictor of radiosensitivity in breast cancer.[5] For the aspect of therapy, zinc finger proteins have been conducted to serve as an anti-viral factor, typically in targeting HIV.[6,7] Another popular target of zinc finger proteins is poly (ADP-ribose)-polymerases (PARPs), as well known, whose inhibitor has been utilized in diverse cancers. In addition, substitution of Zn^{2+} by another metal ion in the zinc fingers emerged as a novel inhibition strategy.[8] Thereby, the zinc finger proteins could be considered as a therapeutic target in human diseases, which deserve in-depth study.

Zinc Finger Protein 536 (ZNF536) gene is located on chromosome 19q12, encoding a highly conserved zinc finger protein with C2H2 domains. It has DNA-binding transcription repressor activity, RNA polymerase II-specific and RNA polymerase II cis-regulatory region sequence-specific DNA binding activity, involving in negative regulation of transcription by RNA polymerase II (https://www.alliancegenome.org/). To date, there are few studies on ZNF536. It was firstly reported as a transcriptional suppressor that negatively regulates neuron differentiation by repressing retinoic acid-induced gene transcription.[9] The specific mechanism was to bind and interrupt RARA from binding to retinoic acid response elements (RARE) composed of tandem 5'-AGGTCA-3' sites known as DR1-DR5.[9] As an important paralog of ZNF536, ZNF516 was found to be a tumor suppressor via blocking the transcription of Sox2 to suppress the proliferation, invasion, and stem cell-like characteristics in colorectal cancer cells.[10] It was also reported that ZNF516 inhibited EGFR transcription by interaction with the complex of CtBP/LSD1/CoREST in breast cancer cells.[11] However, there are no studies focusing on the association between ZNF536 and any cancer so far, let alone pan-cancer analysis.

In this article, we explored the mRNA differential expression and DNA methylation of ZNF536 in pan-cancer and normal controls based on The Cancer Genome Atlas (TCGA) and Genotype Tissue-Expression (GTEx) data. Immunohistochemistry was performed on a tissue micro-array to detect the protein expression of ZNF536. The prognostic implication of ZNF536 in pan-cancer was studied by survival analysis. Then the cBioPortal database was used to display ZNF536 genomic alterations. The co-expression of ZNF536 and immune-related genes in pan-cancer was investigated. Further research was made on the relationship between ZNF536 expression and tumor immune microenvironment. Meanwhile, CancerSEA was employed to excavate the ZNF536 expression at single cell level with different cancer function. Finally, the biological function of ZNF536 in pan-cancer was exhibited by gene enrichment analysis. To the best of our knowledge, it is the first study to elucidate the biologic and prognostic implication for ZNF536 in pan-cancer by comprehensive analysis. The results indicated that ZNF536 might be a prognostic and immune-related biomarker for specific malignancies through the angiogenesis pathway.

Methods

Analysis of Gene Expression and Methylation

UCSC XENA (https://xenabrowser.net/datapages/) RNAseq data in TPM format for TCGA and GTEx were processed uniformly by the Toil 12 to preform group comparison. Pairwise analysis was performed by downloading and collating RNAseq data from the TCGA-ALL (pan-cancer) project STAR process in the TCGA database (https://portal.gdc.cancer.gov). With the exception of missing information and duplicate values, the expression data were transformed using $\log_2$ (value+1). The differential expression was analyzed by R software (version 4.2.1) and visualized by ggplot2 (version 3.3.6). Besides, the distinct expression profiles of ZNF536 between pan-cancer and their adjacent normal tissues were examined using TIMER2.0. The ZNF536 promoter differential methylation in all TCGA cancers was explored using UALCAN. The connection between ZNF536 expression and patients' pathological stage was investigated by GEPIA2.0.

Immunohistochemistry on Tissue Micro-Array

To date, there has been no expression profile of ZNF536 protein in public databases. Herein, the protein expression of ZNF536 was detected by immunohistochemistry on a human tissue micro-array (Cat No. HOrgC120PG04, 5, Shanghai Outdo Biotech Co., Ltd., Shanghai, China). The Ethics Committee of Shanghai Outdo Biotech Co., Ltd. approved the study using those human subjects (No. SHYJS-CP-1901007). The tissue micro-array has a total of 120 points, with a diameter of 1.5 mm of each point. There are 11 kinds of common cancers (2-6 cases per kind) with 1 point each of cancer and its adjacent tissue, and there are 8 kinds of normal human tissues (1-4 cases per kind). The cancers include thyroid papillary carcinoma, esophageal squamous cell carcinoma, stomach adenocarcinoma, colon adenocarcinoma, rectum adenocarcinoma, hepatocellular carcinoma, pancreatic carcinoma, lung squamous

cell carcinoma, lung adenocarcinoma, breast invasive carcinoma, and renal clear cell carcinoma. Normal human tissues include thyroid, esophagus, stomach, colon, rectum, liver, pancreas, and lung. The micro-array was treated with EDTA (pH 9) buffer for heat-mediated antigen retrieval before commencing with the immunohistochemical staining protocol. The primary antibody against ZNF536 (Invitrogen, Catalog # PA5-24338) with a concentration of 5µg/ml (1:100 dilution) was utilized, followed by HRP-conjugated secondary antibody and DAB staining.

Survival Analysis in Pan-Cancer

The mRNA expression of ZNF536 and clinical data in pan-cancer were obtained from TCGA database. The expression was divided into high and low group with a cut-off value of 50%. Cox proportional hazard models with log-rank test and Kaplan-Meier plotter was preformed to evaluate the correlation between ZNF536 expression and patients' prognosis. The survival parameters included overall survival (OS), progress free interval (PFI) and disease specific survival (DSS). Proportional hazard hypothesis testing and fitted survival regression were performed using survival package (version 3.3.1). The results were visualized using the survminer and ggplot2 package (version 3.3.6).

Genomic Alterations

The genomic alterations of ZNF536 in the TCGA pan-cancer datasets were examined using the cBioPortal database (http://www.cbioportal.org/), including alteration frequency, mutation site, mutation types and related genes alteration frequency in ZNF536 altered and unaltered group. The survival analysis for pan-cancer with or without ZNF536 alteration was explored as well. The three-dimensional (3D) candidate protein was conducted using the SWISS-model (https://www.swissmodel.expasy.org) with a UniProt code O15090, and the mutated structure was analyzed and visualized using PyMol (http://www.pymol.org).

Association with Tumor Immune Microenvironment

The prior gene list was obtained from ImmPort (https://www.immport.org/), containing 2483 immune-related genes, involving MHC molecules, immune stimulators, immune inhibitors, chemokines and et al. The R-packages "reshape2" and "RColorBrewer" were used to process the relationship between ZNF536 and immune-related genes. The association between ZNF536 expression and immune infiltration in various TCGA cancers were assess by the TIMER2.0 online tool. Furthermore, Spearman's coefficient was calculated to show the correlation. The absolute value of the coefficient represented the degree of correlation: 0-0.3 represented weak or uncorrelated, 0.3-0.5 represented weak correlation, 0.5-0.8 indicated moderate correlation, and 0.8-1 indicated strong correlation.

Single Cell Sequencing

The CancerSEA database (http://biocc.hrbmu.edu.cn/CancerSEA/) is dedicated to decode multiple functional states of pan-cancer cells at single cell level, which contains angiogenesis, apoptosis, cell cycle, differentiation, DNA damage, DNA repair, epithelial mesenchymal transition (EMT), hypoxia, inflammation, invasion, metastasis, proliferation, quiescence and stemness. Based on the data of single cell sequencing, relevance of ZNF536 across the 14 functional states in distinct cancers was analyzed. The ZNF536 expression distribution of cells were described by T-SNE diagrams.

Gene Enrichment Analysis

Through the use of the R-packages "clusterProfiler", the Gene Set Enrichment Analysis (GSEA) of the biological functions of ZNF536 in pan-cancer was performed. The protein-protein interaction (PPI) network was displayed using BioGRID (https://thebiogrid.org/). The top 100 ZNF536-correlated genes from all TCGA tumor and normal tissues were gathered in GEPIA2.0 website. Then, we used Pearson correlation analysis to determine the relationship between ZNF536 and the chosen genes. To investigate the underlying biological processes and signaling pathways impacted by ZNF536 in TCGA cancers, Gene Ontology (GO) and Kyoto Encyclopedia of Genes and Genomes (KEGG) enrichment analysis were performed as well.

Statistical Analysis

The expression differences were investigated using Wilcoxon rank sum test. While the correlations between two groups were evaluated by Spearman rank test. Kaplan-Meier survival curves were used to examine the prognosis using log-rank test and Cox regression model by calculating the hazard ratio. P-values less than 0.05 were considered statistically significant.

Results

Differential mRNA Expression and DNA Methylation of ZNF536 in Pan-Cancer

Differential expression analysis of ZNF536 mRNA based on TCGA and GTEx data demonstrated that there were significant differences in various cancers and their normal or adjacent tissues (Figure 1A and Supplementary Figure S1A). Analysis by TIMER2.0 obtained the similar results (Figure 1B). The highly expressed ZNF536 was in kidney chromophobe (KICH), pancreatic adenocarcinoma (PAAD), thymoma (THYM), and uterine carcinosarcoma

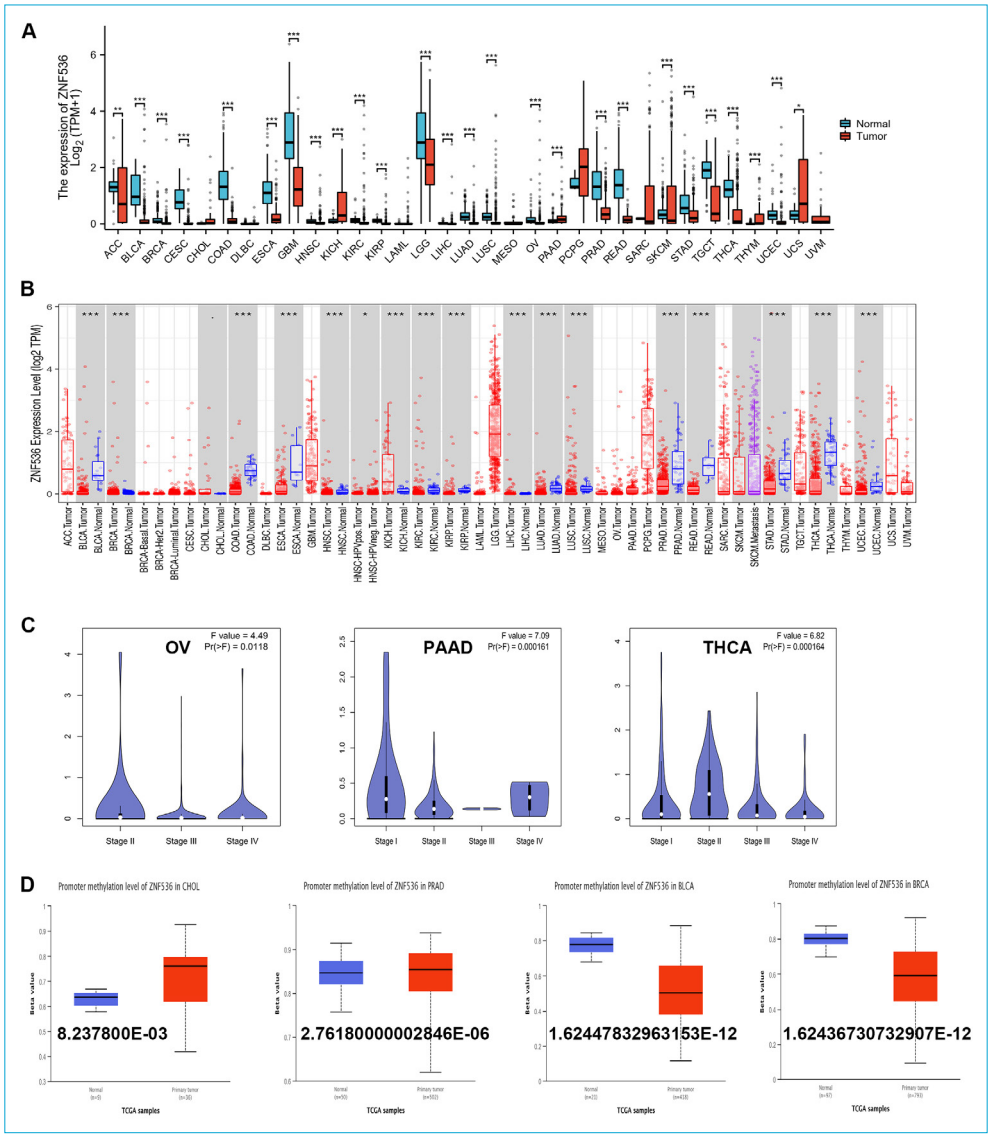

Figure 1. Differential mRNA expression and DNA methylation of ZNF536 in pan-cancer. Differential expression of ZNF536 mRNA based on TCGA and GTEx data **(a)**. ZNF536 mRNA expression in different cancer types in TIMER **(b)**. ZNF536 expression levels and the pathological stages were analyzed using GEPIA2.0 **(c)**. Promoter methylation values of ZNF536 between normal and primary tumor tissues were analyzed using UALCAN **(d)**. * represented p<0.05, ** represented p<0.01, and *** represented p<0.001.

(UCS). Whereas, in adrenocortical carcinoma (ACC), bladder urothelial carcinoma (BLCA), breast invasive carcinoma (BRCA), cervical endocervical adenocarcinoma and squamous cell carcinoma (CESC), colon adenocarcinoma (COAD), esophageal carcinoma (ESCA), glioblastoma multiforme (GBM), head and neck squamous cell carcinoma (HNSC), kidney renal clear cell carcinoma (KIRC), kidney renal papillary cell carcinoma (KIRP), brain lower grade glioma (LGG), liver hepatocellular carcinoma (LIHC), lung adenocarcinoma (LUAD), lung squamous cell carcinoma (LUSC), ovarian serous cystadenocarcinoma (OV), prostate adenocarcinoma (PRAD), rectum adenocarcinoma (READ), skin cutaneous melanoma (SKCM), stomach adenocarcinoma (STAD), testicular germ cell tumors (TGCT), thyroid carcinoma (THCA), and uterine corpus endometrial carcinoma (UCEC), it was decreased (Supplementary Figure S1B). We further investigated the relationship between the level of ZNF536 mRNA and the pathological stages of cancers using GEPIA2.0. In OV, PAAD, and THCA, we found obvious impact of ZNF536 mRNA expression on the patients' stages (Figure 1C). The promoter methylation levels of ZNF536 in pan-cancer were explored by UALCAN online tool. The DNA methylation was significantly elevated in cholangiocarcinoma (CHOL) and PRAD, while declined

in BLCA, BRCA, COAD, KIRC, KIRP, LUAD, LUSC, pheochromocytoma and paraganglioma (PCPG), and READ (Figure 1D and Supplementary Figure S1C).

Protein Expression of ZNF536 in Multiple Cancer Tissues

Due to the limitation of sample size, there were statistical significance in only two cancer types, as shown in Table 1. The ZNF536 expression was significantly decreased in STAD (n=5) compared with its adjacent tissue, while significantly increased in PAAD (n=4) (Figure 2A-B). ZNF536 was also found to be expressed in a considerable number of specific cancer types, including THCA (n=3), COAD (n=6), READ (n=4), LIHC (n=6), LUAD (n=6) and KIRC (n=5), with no discernible difference (Figure 2C-H). In ESCA (n=4) and LUSC (n=4), it showed low expression without significance as well (Figure 2I-J). The results of 18 normal tissues exhibited that ZNF536 was expressed in thyroid (n=4), stomach (n=2), colon (n=2), liver (n=1), pancreas (n=1), and lung (n=4), while was not expressed in esophagus (n=2) and rectum (n=2) (Supplementary Figure S2A-H).

Table 1. The protein expression of ZNF536 in pan-cancer on a tissue micro-array

Cancer type	n	Expression		p
		Positive	Negative	
THCA				>0.9999 (ns)
cancer	3	3	0	
adjacent	3	3	0	
ESCC				>0.9999 (ns)
cancer	4	1	3	
adjacent	4	2	2	
STAD				0.0286 (*)
cancer	4	0	4	
adjacent	4	4	0	
COAD				0.5455 (ns)
cancer	6	5	1	
adjacent	6	3	3	
READ				>0.9999 (ns)
cancer	4	3	1	
adjacent	4	2	2	
LIHC				>0.9999 (ns)
cancer	6	6	0	
adjacent	6	6	0	
PAAD				0.0476 (*)
cancer	5	5	0	
adjacent	5	1	4	
LUSC				>0.9999 (ns)
cancer	4	0	4	
adjacent	4	0	4	
LUAD				>0.9999 (ns)
cancer	6	5	1	
adjacent	6	5	1	
KIRC				>0.9999 (ns)
cancer	5	5	0	
adjacent	5	4	1	
Normal tissue	18	14	4	NA

Fisher's exact test was applied to compare ZNF536 expression between cancer and adjunct tissue. n represented number of cases, ns represented no statistical significance, * represented p<0.05.

Prognostic Prediction of ZNF536 in Pan-Cancer

The OS, PFI and DSS were assessed to display the patients' prognosis in pan-cancer. High expression of ZNF536 mRNA corresponded shorter OS, PFI and DSS in ACC (OS: p=0.016, HR=2.74; PFI: p=0.013, HR=3.02; DSS: p=0.006, HR=2.50), KIRP (OS: p=0.017, HR=2.12; PFI: p=0.009, HR=2.99; DSS: p=0.008, HR=2.08) and uveal melanoma (UVM) (OS: p=0.008, HR=3.34; PFI: p=0.008, HR=3.61; DSS: p=0.006, HR=3.00) (Figure 3A-C). In KIRC (OS: p=0.016, HR=1.45; PFI: p=0.085, HR=1.40; DSS: p=0.413, HR=1.14) and oral squamous cell carcinoma (OSCC) (OS: p=0.028, HR=1.44; PFI: p=0.068, HR=1.47; DSS: p=0.126, HR=1.30), the expression level was only significantly associated with OS (Supplementary Figure S3A-B). On the contrary, high expression of ZNF536 mRNA predicted favorable prognosis with lengthened OS, PFI and DSS in GBMLGG (OS: p=0.011, HR=0.73; PFI: p=0.017, HR=0.74; DSS: p=0.007, HR=0.75) (Figure 3D), and with lengthened OS and DSS in PRAD (OS: p=0.040, HR=0.11; PFI: p=0.999, HR=0.00; DSS: p=0.006, HR=0.56) (Supplementary Figure S3C). The Cox proportional hazards model of ZNF536 mRNA expression in pan-cancer was summarized and listed in Table 2.

Genomic Alterations of ZNF536 in Pan-Cancer

The genomic alterations of ZNF536 were explored using cBioPortal with data based on TCGA, PanCancer Atlas. The highest frequency of amplification (31.58%) was in UCS, and the highest frequency of mutation (20.32%) was in LUAD (Figure 4A). The most mutation type was missense, followed by truncating, splice and SV/fusion (Figure 4B). A missense mutation of E549K was detected in 2 UCECs and 4 SKCMs. The wild-type and mutated ZNF536 were modeled by PyMol which showed no effect of E549K residue change on the polar contact with their around amino acid N547 (Figure 4C). The main putative copy-number alterations of ZNF536 were diploid, shallow deletion and gain (Supplementary Figure S4A). Compared with unaltered group, the alteration frequency of MFSD13B, TP53, TTN, MUC16, CSMD3, LRP1B, URI1, CCNE1, TSHZ3, and RYR2 were elevated obviously in ZNF536 altered group (Figure 4D). Moreover, the OS and PFI were slightly lower in altered group

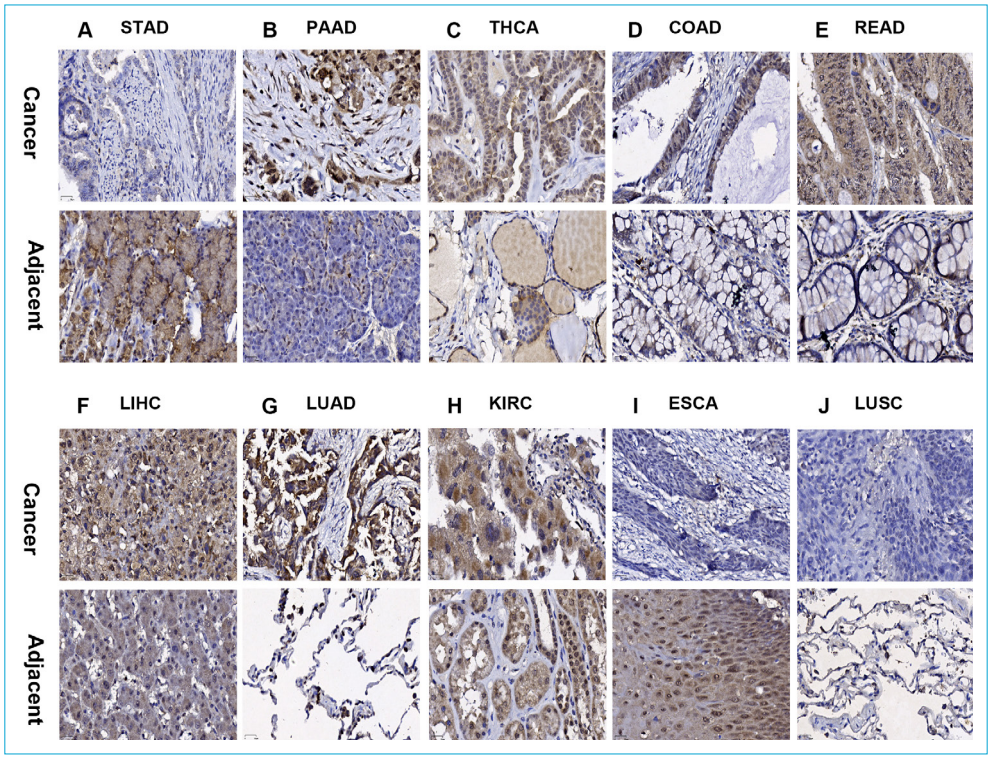

Figure 2. Protein expression of ZNF536 in multiple cancer tissues of STAD **(a)**, PAAD **(b)**, THCA **(c)**, COAD **(d)**, READ **(e)**, LIHC **(f)**, LUAD **(g)**, KIRC **(h)**, ESCA **(i)** and LUSC **(j)**. They were all originally magnified principal images (×200) with a scale bar of 30μm.

than unaltered group (Supplementary Figure S4B).

Relationship Between ZNF536 Expression and Tumor Immune Microenvironment

Through investigating the co-expression of ZNF536 and immune-related genes, we found that the majority of immune-related genes and ZNF536 mRNA expression level were highly associated, suggesting that ZNF536 may play a role in mediating immune escape. The mRNA expression of ZNF536 was observed to be linked with at least 30 immune-related genes, including TNFRSF9, CD86, TIGIT, TNFSF15, BTNL2, TNFSF14, CD80, CTLA4, CD40LG, ICOS, LAIR1 and NRP1, in COAD, PRAD, TGCT and THCA (Supplementary Figure S5A). There were correlations of ZNF536 mRNA expression with immune infiltration levels in diverse cancer types. In BRCA, CESC, HNSC, KIRC, KIRP, LUSC, PRAD, THYM, and UCEC, the mRNA expression of ZNF536 was positively correlated with infiltration of cancer associated fibroblasts predominantly (Supplementary Figure S5B). Other obvious positive correlations were observed with Tregs and B cells both in COAD and ESCA (Supplementary Figure S5B). In UVM, ZNF536 mRNA expression was positively correlated with most immune infiltrates, among which the coefficient (R=0.590) of Tgd was the highest (Supplementary Figure S5C). While in ACC, the relationship was negative in most immune infiltrates, with the lowest coefficient (R=-0.580) of immature dendritic cells (iDC) (Supplementary Figure S5C). Furthermore, there were 16 types of immune infiltrates related with ZNF536 mRNA expression in ACC, 12 in PRAD, 7 in PAAD, and 7 in UCS (Figure 5). In the rest cancers, the related cell types were less than 5, or had no statistical significance.

Analysis of ZNF536 at Single Cell Level

As remarkably exhibited by the heat map (Figure 6A), the ZNF536 mRNA expression was positively related with angiogenesis and differentiation, while negatively related with apoptosis, cell cycle, DNA damage, DNA repair, EMT, hypoxia, invasion, metastasis, quiescence and stemness in GBM. In retinoblastoma (RB), there were positive correlations between ZNF536 mRNA expression and angiogenesis, differentiation, inflammation, metastasis, quiescence and stemness, and there were negative correlations between ZNF536 mRNA expression and apoptosis, cell cycle, DNA damage, DNA repair and invasion. The substantial association between the mRNA expression of ZNF536 and invasion and DNA repair in GBM, angiogenesis, differentiation, inflammation, DNA repair, DNA damage, and cell cycle in RB, DNA repair and apop-

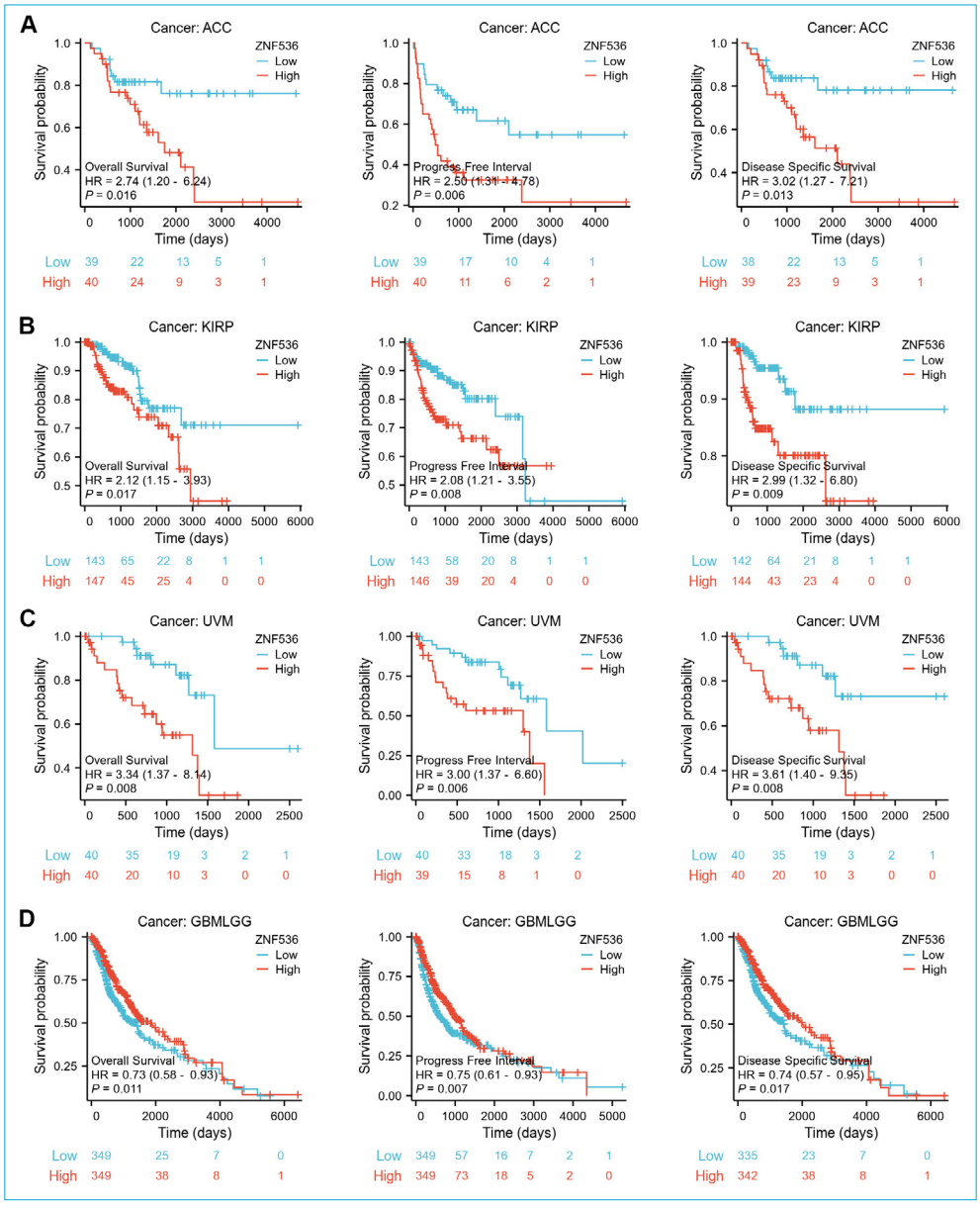

Figure 3. Survival analysis of ZNF536 in pan-cancer. ZNF536 mRNA was negatively associated with OS, PFI and DSS in ACC **(a)**, KIRP **(b)** and UVM **(c)**. High expression of ZNF536 mRNA predicted favorable prognosis with lengthened OS, PFI and DSS in GBMLGG **(d)**.

tosis in UM, and quiescence, differentiation, cell cycle and proliferation in acute lymphoblastic leukemia (ALL) was shown in Supplementary Figure S6A-D. In addition, ZNF536 mRNA expression profiles from GBM, RB, UM, and ALL single cells were displayed by T-SNE diagrams (Figure 6B).

Biological Function of ZNF536 in Pan-Cancer

The primary biological pathways in pan-cancer impacted by ZNF536 was investigated using GSEA. Given GO analysis, we found that ZNF536 positively regulated signaling pathways in ACC, BLCA, BRCA, COAD, DLBL, ESCA, HNSC, KIRC, KIRP, LIHC, LUAD, LUSC, SARC, STAD, UCEC, and UVM, while negatively regulated signaling pathways in LGG, MESO, OV, and THCA (Figure 7A-H). The main biological pathways of ZNF536 involved in pan-cancer included artery morphogenesis, mRNA cis splicing via spliceosome, protein localization to cell surface, cholesterol metabolic process, endothelial cell differentiation, immunoglobulin complex, cardiac muscle tissue development, and so on. In addition, the network of ZNF536 and its related genes was displayed using BioGRID online tool (Supplementary Figure S7A). 10 of top 100 ZNF536 related genes, AATK, PLP1, CNTN2, CNP, MOG, ERMN, GPR62, PRR18, MBP, and

Table 2. Cox proportional hazards model of ZNF536 mRNA expression in pan-cancer

Cancer	OS		DSS		PFI	
	p	HR	p	HR	p	HR
ACC	0.016	2.74 (1.20–6.24)	0.013	3.02 (1.27–7.21)	0.006	2.50 (1.31–4.78)
BLCA	0.806	1.04 (0.77–1.39)	0.353	1.18 (0.83–1.68)	0.418	1.13 (0.84–1.51)
BRCA	0.736	0.95 (0.69–1.30)	0.302	1.25 (0.82–1.92)	0.271	1.20 (0.87–1.66)
CESC	0.640	0.90 (0.56–1.42)	0.289	0.75 (0.44–1.28)	0.520	0.86 (0.54–1.36)
CHOL	0.839	1.10 (0.42–2.88)	0.846	1.11 (0.40–3.07)	0.900	0.95 (0.39–2.27)
COAD	0.177	0.76 (0.51–1.13)	0.254	0.75 (0.45–1.23)	0.694	0.93 (0.66–1.32)
COADREAD	0.285	0.83 (0.58-1.17)	0.310	0.79 (0.51-1.24)	0.580	1.09 (0.80-1.48)
DLBC	0.244	0.38 (0.07–1.95)	0.885	0.87 (0.12–6.17)	0.118	0.33 (0.08–1.33)
ESAD	0.646	0.86 (0.46-1.62)	0.969	0.99 (0.47-2.07)	0.530	0.82 (0.45-1.51)
ESCA	0.387	0.81 (0.49–1.31)	0.314	0.74 (0.42–1.32)	0.922	0.98 (0.63–1.52)
ESCC	0.368	0.69 (0.31-1.54)	0.120	0.44 (0.16-1.24)	0.482	1.26 (0.66-2.41)
GBM	0.868	1.03 (0.73–1.44)	0.830	1.04 (0.73–1.49)	0.674	0.93 (0.66-1.30)
GBMLGG	0.011	0.73 (0.58-0.93)	0.017	0.74 (0.57-0.95)	0.007	0.75 (0.61-0.93)
HNSC	0.163	1.21 (0.93–1.58)	0.240	1.23 (0.87–1.74)	0.158	1.23 (0.92–1.63)
KICH	0.900	1.09 (0.29–4.05)	0.855	1.15 (0.26–5.14)	0.409	1.68 (0.49–5.74)
KIRC	0.016	1.45 (1.07–1.95)	0.085	1.40 (0.95–2.04)	0.413	1.14 (0.83–1.55)
KIRP	0.017	2.12 (1.15–3.93)	0.009	2.99 (1.32–6.80)	0.008	2.08 (1.21–3.55)
LAML	0.484	0.86 (0.56–1.31)	/	/	/	/
LGG	0.133	1.30 (0.92–1.82)	0.142	1.31 (0.91–1.87)	0.075	1.28 (0.98–1.68)
LUAD	0.081	0.77 (0.58–1.03)	0.171	0.77 (0.54–1.12)	0.353	0.88 (0.68–1.15)
LUSC	0.961	1.01 (0.77–1.32)	0.711	0.92 (0.61–1.41)	0.859	0.97 (0.70–1.34)
LUADLUSC	0.217	0.88 (0.73-1.08)	0.218	0.84 (0.64-1.11)	0.653	0.95 (0.78-1.17)
MESO	0.614	1.13 (0.70–1.82)	0.914	0.97 (0.53–1.77)	0.348	0.78 (0.47–1.31)
OSCC	0.028	1.44 (1.04–1.99)	0.068	1.47 (0.97–2.21)	0.126	1.30 (0.93–1.83)
OV	0.120	1.23 (0.95-1.59)	0.104	1.26 (0.95-1.66)	0.829	1.03 (0.81-1.30)
PAAD	0.102	0.71 (0.47–1.07)	0.291	0.78 (0.49–1.24)	0.268	0.81 (0.55–1.18)
PCPG	0.563	1.53 (0.36–6.40)	0.165	4.58 (0.53–39.28)	0.674	0.84 (0.36–1.94)
PRAD	0.040	0.11 (0.01–0.91)	0.999	0.00 (0.00–Inf)	0.006	0.56 (0.37–0.85)
READ	0.148	0.55 (0.24–1.24)	0.475	0.68 (0.24–1.96)	0.652	1.16 (0.61–2.22)
SARC	0.061	1.46 (0.98–2.18)	0.095	1.45 (0.94–2.24)	0.411	1.15 (0.83–1.60)
SKCM	0.790	1.04 (0.79–1.36)	0.592	1.08 (0.81–1.44)	0.786	1.03 (0.82-1.29)
STAD	0.715	1.06 (0.77–1.47)	0.502	1.15 (0.76–1.75)	0.117	1.33 (0.93–1.89)
TGCT	0.999	0.00 (0.00–Inf)	0.999	0.00 (0.00–Inf)	0.793	1.09 (0.58–2.03)
THCA	0.354	1.60 (0.59–4.32)	/	/	0.119	0.65 (0.37–1.12)
THYM	0.225	0.38 (0.08–1.83)	0.488	0.45 (0.05–4.35)	0.420	1.43 (0.60-3.38)
UCEC	0.347	1.21 (0.81–1.82)	0.252	1.34 (0.81–2.20)	0.843	0.97 (0.68–1.36)
UCS	0.329	0.70 (0.35–1.43)	0.688	0.86 (0.41–1.80)	0.320	0.72 (0.37–1.38)
UVM	0.008	3.34 (1.37–8.14)	0.008	3.61 (1.40–9.35)	0.006	3.00 (1.37-6.60)

OS: Overall Survival; DSS: Disease Specific Survival; PFI: Progress Free Interval. p: p value; HR: Hazard Ratio.

MAG, demonstrated strong correlations with ZNF536 in the majority of cancer types (Supplementary Figure S7B). The biological functions of the co-expressed genes for ZNF536 in the control of axon development, axon genesis and neuronal cell body were revealed by GO and KEGG enrichment analysis (Supplementary Figure S7C).

Discussion

ZNF536 was firstly discovered by Qin et al.,[9] as a novel zinc finger protein, it is expressed in the brain exclusively, suppressing retinoic acid-induced gene transcription to adversely regulate neuron development. At present, research on ZNF536 is very rare, most of them focus on neurology

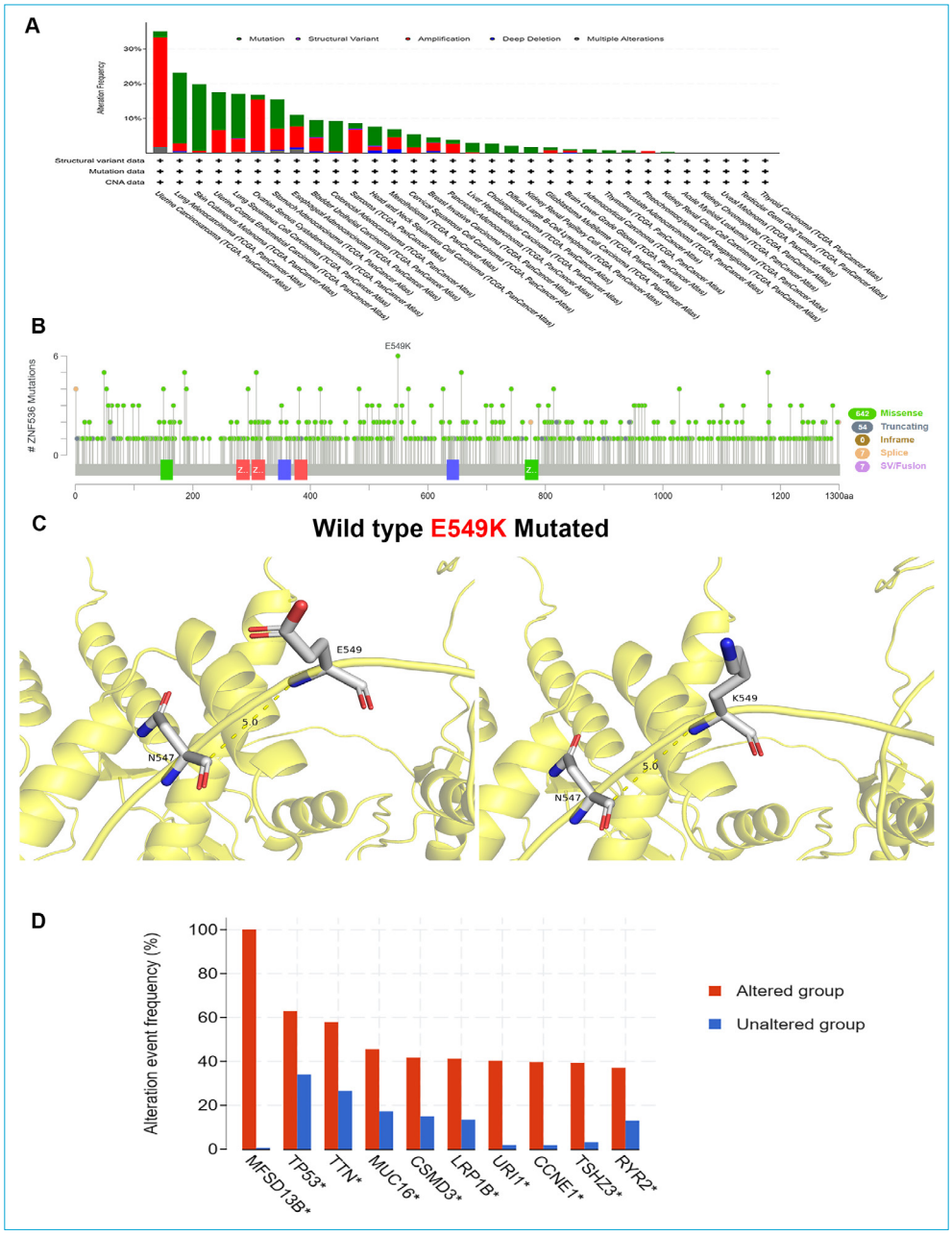

Figure 4. Genomic alterations of ZNF536 in pan-cancer. Alterations summary of ZNF536 **(a)** and mutation sites **(b)**. Wild and mutated types of the p.E549K variant compared by PyMol **(c)**. The alteration event frequency of related genes in ZNF536 altered group and unaltered group **(d)**. * represented $p<0.05$.

and psychiatry. Single cell RNA sequencing[13] revealed the important role of ZNF536 as a transcription factor in the development of forebrain neurons involved in social behavior and stress. Single nucleotide polymorphisms (SNPs) studies [14] have shown that ZNF536 rs2053079 was associated with schizophrenia risk, while ZNF536 rs77554113 was associated with antidepressant remission.[15] However, the role of ZNF536 in any cancer or even pan-cancer remains unknown, which worth exploring. As a result, we created the research focuing on ZNF536's activities in human pan-cancer in this work. The ZNF536 mRNA was highly expressed in KICH, PAAD, THYM, and UCS, but lowly expressed in ACC, BLCA, BRCA, CESC, COAD, ESCA, GBM, HNSC, KIRC, KIRP, LGG, LIHC, LUAD, LUSC, OV, PRAD, READ, SKCM, STAD, TGCT, THCA, and UCEC. The immunohistochemistry on the tissue micro-array confirmed the high expression of ZNF536 protein in PAAD and low expression in STAD with statistical significance, and low expression in ESCA and LUSC with-

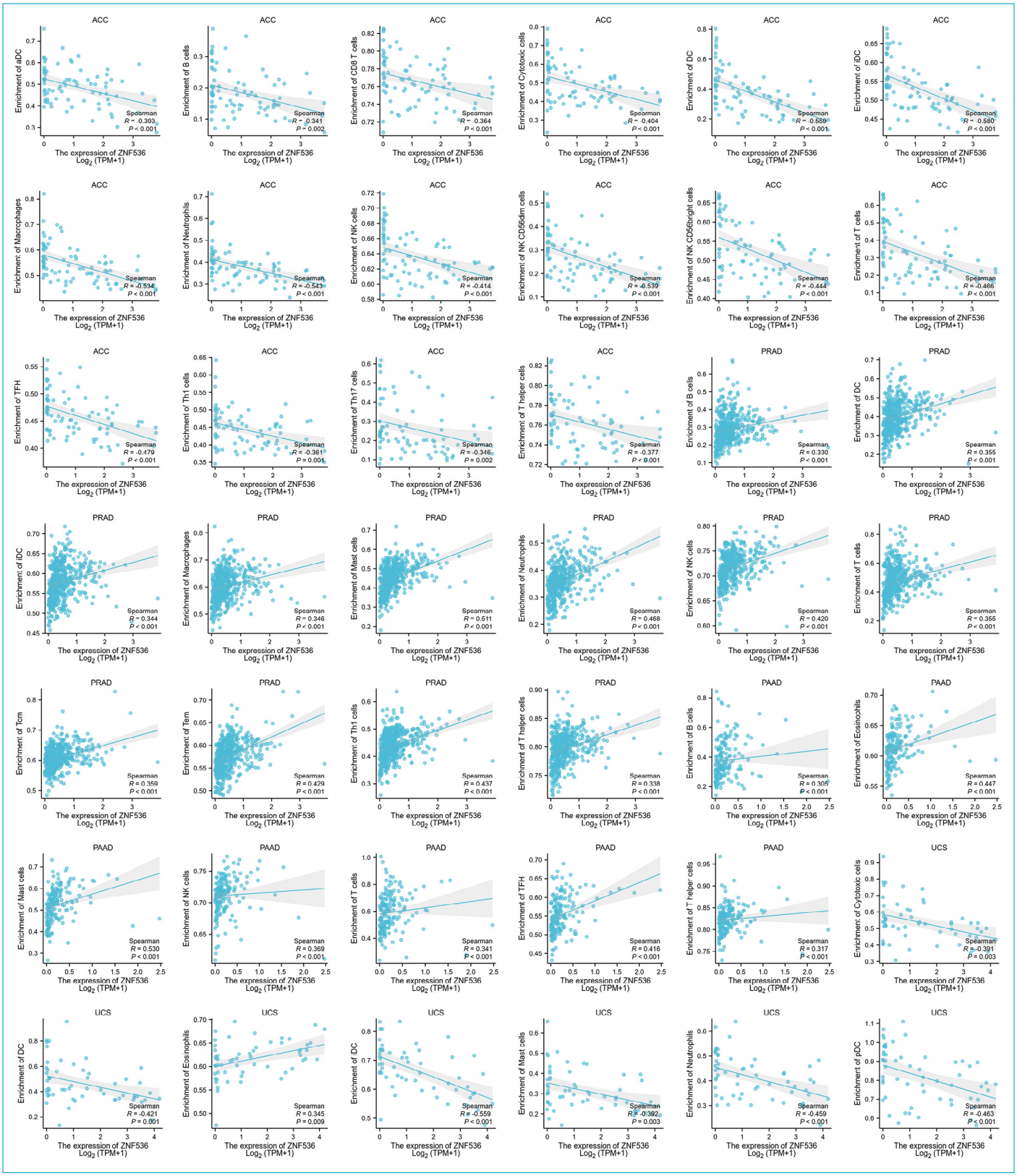

Figure 5. Relationship between ZNF536 mRNA expression and various immune infiltrates in pan-cancer.

out statistical significance. It might be attributed to the not enough large sample size, which could be altered by expand the sample scale. Besides, the protein expression trend was not consistent with its mRNA in the rest cancers, which might result from post-transcriptional modification processes[16] The differential expression of ZNF536 mRNA

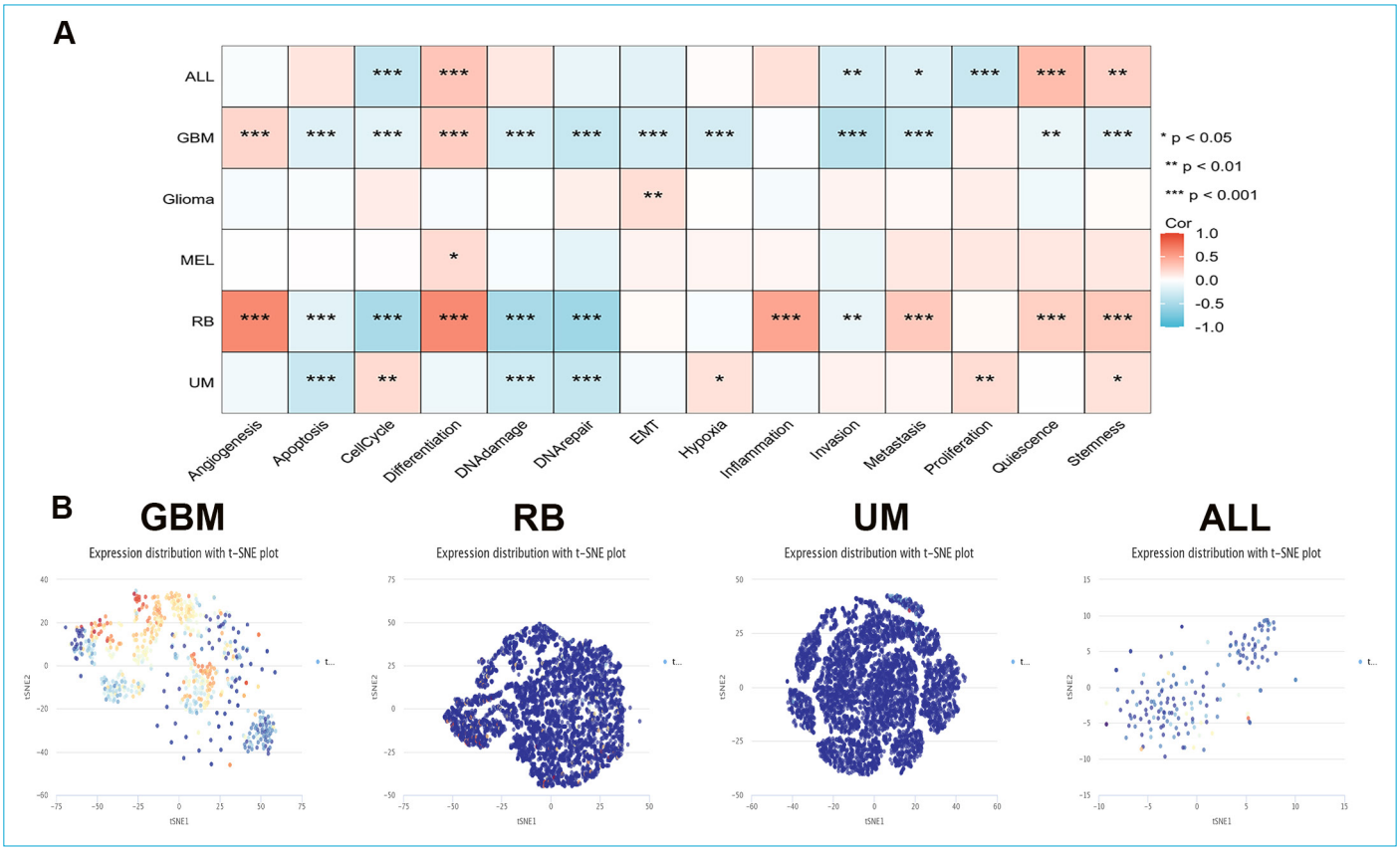

Figure 6. Analysis of ZNF536 at single cell level. The association between ZNF536 mRNA expression and various functional states in cancers **(a)**. ZNF536 mRNA expression profiles from GBM, RB, UM, and ALL single cells were displayed by T-SNE diagrams **(b)**. * represented p<0.05, ** represented p<0.01, and *** represented p<0.001.

in OV, PAAD and THCA with different pathological stages indicated that there was an obvious impact of ZNF536 on the patients' stages. Furthermore, DNA hypermethylation in CHOL and PRAD, and hypomethylation in BLCA, BRCA, COAD, KIRC, KIRP, LUAD, LUSC, PCPG and READ were observed. Considering the mRNA expression level, promoter hypermethylation of ZNF536 might be a driver of down-regulated expression in PRAD.

As displayed by the Kaplan-Meier curves, ZNF536 mRNA was negatively associated with OS, PFI and DSS in ACC, KIRP and UVM, and with OS in KIRC and OSCC. It demonstrated that ZNF536 might serve as a predictor for poor prognosis in those cancers. Whereas high expression of ZNF536 mRNA predicted favorable prognosis in GBMLGG and PRAD. Meanwhile, the mRNA expression of ZNF536 was verified to be a lower level in PRAD compared to its normal tissue. We deduced that it might exert the function of tumor suppressor gene in PRAD. According to a recent study,[17] another zinc finger protein, ZFC3H1, was identified to be a potential marker for the prognosis of PRAD. ZFC3H1 expression in PRAD were significantly lower than that in the corresponding adjacent tissues, and patients in the high ZFC3H1-expression group had poor prognosis. Reduced ZFC3H1 inhibited PRAD cell viability, cell migration and invasion, and increased cell apoptosis, which further clarified the suppressor role of ZFC3H1 in PRAD. As an analogue of ZFC3H1, if ZNF536 have the same function in PRAD needs to be investigated in the future.

By exploring genomic alterations of ZNF536 using cBioPortal, we found that the highest frequency was amplification, followed by mutation in pan-cancer. Amplification might contribute to the elevated gene expression in certain cancers. For the missense mutation of E549K, it caused glutamic acid at position 549 of the ZNF536 protein substituted by lysine, which not located in the crucial C2H2 domain, indicating that there might be no influence on protein function. It was also found that the alteration frequency of MFSD13B, TP53, TTN, MUC16, CSMD3, LRP1B, URI1, CCNE1, TSHZ3, and RYR2 were elevated obviously in ZNF536 altered group. Among them, TP53 and LRP1B were recognized as tumor suppressors in several cancers, associating with immune response in LUSC and HCC.[18,19] It might be a factor for the worse prognosis in the altered group than in the unaltered group.

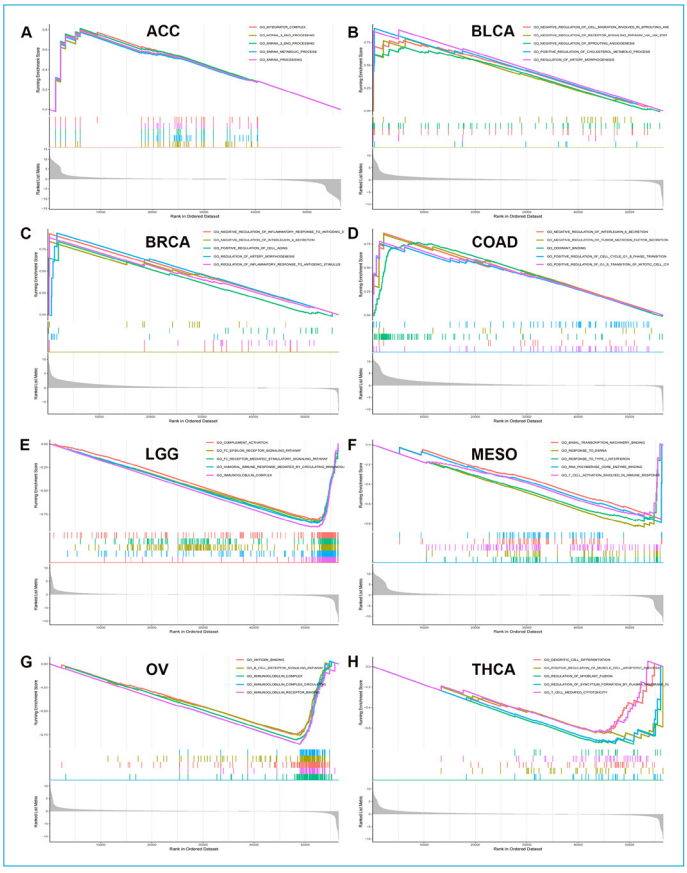

Figure 7. GSEA analysis in GO signature of ZNF536 in ACC **(a)**, BLCA **(b)**, BRCA **(c)**, COAD **(d)**, LGG **(e)**, MESO **(f)**, OV **(g)**, and THCA **(h)**.

In recent years, the tumor microenvironment has been the subject of considerable research, particularly the immune microenvironment. In this study, at least 30 immune-related genes were shown to be associated with ZNF536 mRNA expression in COAD, PRAD, TGCT, and THCA, including TNFRSF9, CD86, TIGIT, TNFSF15, BTNL2, TNFSF14, CD80, CTLA4, CD40LG, ICOS, LAIR1, and NRP1. The strong correlation indicated a potential role of ZNF536 involved in mediating immunological escape. Furthermore, multiple immune cells infiltration was found to be related with ZNF536 mRNA expression, including cancer associated fibroblasts, Tregs, B cells, and so on. For PRAD, there were 12 significantly related immune infiltrates, containing mast cells, neutrophils, Th1 cells, Tem, NK cells, Tcm, T cells, DC, macrophages, iDC, T helper cells, and B cells. Although the results indicated that ZNF536 might be a useful target for immunotherapy, the specific function of ZNF536 in human immune system is still unknown, which warrants further preclinical and clinical trials studied intensively.

Single cell sequencing revealed that the ZNF536-correlated genes might regulate a variety of biological processes in pan-cancer, mainly involving angiogenesis, apoptosis, cell cycle, differentiation, DNA damage, DNA repair, EMT, hypoxia, inflammation, invasion, metastasis, proliferation, quiescence and stemness. Additionally, gene enrichment analysis revealed that ZNF536 regulated distinct signaling pathways in various cancers. Artery morphogenesis, mRNA cis splicing via spliceosome, protein localization to cell surface, cholesterol metabolic process, endothelial cell differentiation, immunoglobulin complex, and cardiac muscle tissue development were identified as the prominent signaling pathways, among which artery morphogenesis and endothelial cell differentiation was associated with angiogenesis. ZNF580, another zinc finger protein, through regulating the expression of VEGF and MMP-2 to promote migration and proliferation of EAhy926 endothelial cells, thus controlled angiogenesis.[20] Its function of pro-angiogenesis has been tried to therapy hindlimb ischemia even more.[21] Therefore, we hypothesize that ZNF536 may be used as a target for anti-angiogenic therapy in cancers, which needs to be confirmed by further studies. In addition, GO and KEGG enrichment studies indicated the biological functions of the co-expressed genes for ZNF536 in the regulation of axon formation, axon genesis, and neuronal cell body, which was basically consistent with previous studies in neurodevelopment.[9]

Conclusion

In this study, we comprehensively explored the biologic and prognostic implication of ZNF536 in pan-cancer by multi-layered analysis of differential mRNA expression and DNA methylation, protein expression on a tissue micro-array, outcomes, genomic alterations, tumor immune microenvironment, single cell sequencing, and signaling pathways enrichment. As the first work to investigate the role of ZNF536 in cancers, it illustrated that ZNF536 might be a potential prognostic and immune-related biomarker for certain cancers via angiogenesis pathway. This study establishes the groundwork for future investigations into the precise mechanisms of ZNF536 in the tumorigenesis and therapeutic regimens of various cancers.

Disclosures

Ethics Committee Approval: This study conforms to the principles outlined in the Declaration of Helsinki (World Medical Association Declaration of Helsinki). The Ethics Committee of Shanghai Outdo Biotech Co., Ltd. approved the study using those human subjects (No. SHYJS-CP-1901007). Written informed consent was obtained.

Peer-review: Externally peer-reviewed.

Conflict of Interest: None declared.

Funding: This study was supported by Anhui Provincial Children's Hospital Excellent Discipline Talent Training Program (eyrc007).

Authorship Contributions: Concept – Y.F.; Design – Q.W.; Supervision – Q.W.; Materials – Y.F.; Data collection &/or processing – Y.F., S.-J.W.; Analysis and/or interpretation – Y.F., S.-J.W.; Literature search – Y.F.; Writing – Y.F.; Critical review – Q.W.

References

1. Jen J, Wang YC. Zinc finger proteins in cancer progression. J Biomed Sci 2016;23:53.
2. Xia L, Lin H, Zhou Y, Lian J. ZNF750 facilitates carcinogenesis via promoting the expression of long non-coding RNA CYTOR and influences pharmacotherapy response in colon adenocarcinoma. J Zhejiang Univ Sci B 2022;23:587–96.
3. He L, Fan X, Li Y, Chen M, Cui B, Chen G, et al. Overexpression of zinc finger protein 384 (ZNF 384), a poor prognostic predictor, promotes cell growth by upregulating the expression of Cyclin D1 in Hepatocellular carcinoma. Cell Death Dis 2019;10:444.
4. Chen X, Liu C, Zhang Z, Wang M, Guo S, Li T, et al. ZNF655 Promotes the progression of glioma through transcriptional regulation of AURKA. Front Oncol 2022;12:770013.
5. Yan D, Shen M, Du Z, Cao J, Tian Y, Zeng P, et al. Developing ZNF gene signatures predicting radiosensitivity of patients with breast cancer. J Oncol 2021;2021:9255494.
6. Iraci N, Tabarrini O, Santi C, Sancineto L. NCp7: targeting a multitask protein for next-generation anti-HIV drug development part 2. Noncovalent inhibitors and nucleic acid binders. Drug Discov Today 2018;23:687–95.
7. Sancineto L, Iraci N, Tabarrini O, Santi C. NCp7: targeting a multitasking protein for next-generation anti-HIV drug development part 1: covalent inhibitors. Drug Discov Today 2018;23:260–71.
8. Abbehausen C. Zinc finger domains as therapeutic targets for metal-based compounds - an update. Metallomics 2019;11:15–28.
9. Qin Z, Ren F, Xu X, Ren Y, Li H, Wang Y, et al. ZNF536, a novel zinc finger protein specifically expressed in the brain, negatively regulates neuron differentiation by repressing retinoic acid-induced gene transcription. Mol Cell Biol 2009;29:3633–43.
10. E J, Kang Z, Yuan J, Wang Z, Tong D, Xing J. ZNF516 suppresses stem cell-like characteristics by regulating the transcription of Sox2 in colorectal cancer. Am J Cancer Res 2022;12:3745–59.
11. Li L, Liu X, He L, Yang J, Pei F, Li W, et al. ZNF516 suppresses EGFR by targeting the CtBP/LSD1/CoREST complex to chromatin. Nat Commun 2017;8:691
12. Vivian J, Rao AA, Nothaft FA, Ketchum C, Armstrong J, Novak A, et al. Toil enables reproducible, open source, big biomedical data analyses. Nat Biotechnol 2017;35:314–6.
13. Thyme SB, Pieper LM, Li EH, Pandey S, Wang Y, Morris NS, et al. Phenotypic landscape of schizophrenia-associated genes defines candidates and their shared functions. Cell 2019;177:478–91.e20.
14. Wang D, Guo T, Guo Q, Zhang S, Zhang J, Luo J; GeseDNA Research Team. The association between schizophrenia risk variants and creativity in healthy Han Chinese subjects. Front Psychol 2019;10:2218.
15. Lin E, Kuo PH, Liu YL, Yu YW, Yang AC, Tsai SJ. A deep learning approach for predicting antidepressant response in major depression using clinical and genetic biomarkers. Front Psychiatry 2018;9:290.
16. Barbieri I, Kouzarides T. Role of RNA modifications in cancer. Nat Rev Cancer 2020;20:303–22.
17. Huang H, Xu H, Li P, Ye X, Chen W, Chen W, et al. Zinc finger C3H1 domain-containing protein (ZFC3H1) evaluates the prognosis and treatment of prostate adenocarcinoma (PRAD): A study based on TCGA data. Bioengineered 2021;12:5504–15.
18. Yu J, Fan Z, Zhou Z, Zhang P, Bai J, Li X, et al. TP53 and LRP1B co-wild predicts improved survival for patients with LUSC receiving anti-PD-L1 immunotherapy. Cancers (Basel) 2022;14:3382.
19. Shi L, Cao J, Lei X, Shi Y, Wu L. Multi-omics data identified TP53 and LRP1B as key regulatory gene related to immune phenotypes via EPCAM in HCC. Cancer Med 2022;11:2145–58.
20. Sun HY, Wei SP, Xu RC, Xu PX, Zhang WC. Sphingosine-1-phosphate induces human endothelial VEGF and MMP-2 production via transcription factor ZNF580: novel insights into angiogenesis. Biochem Biophys Res Commun 2010;395:361–6.
21. Wang X, Su B, Gao B, Zhou J, Ren XK, Guo J, et al. Cascaded bio-responsive delivery of eNOS gene and ZNF580 gene to collaboratively treat hindlimb ischemia via pro-angiogenesis and anti-inflammation. Biomater Sci 2020;8:6545–60.

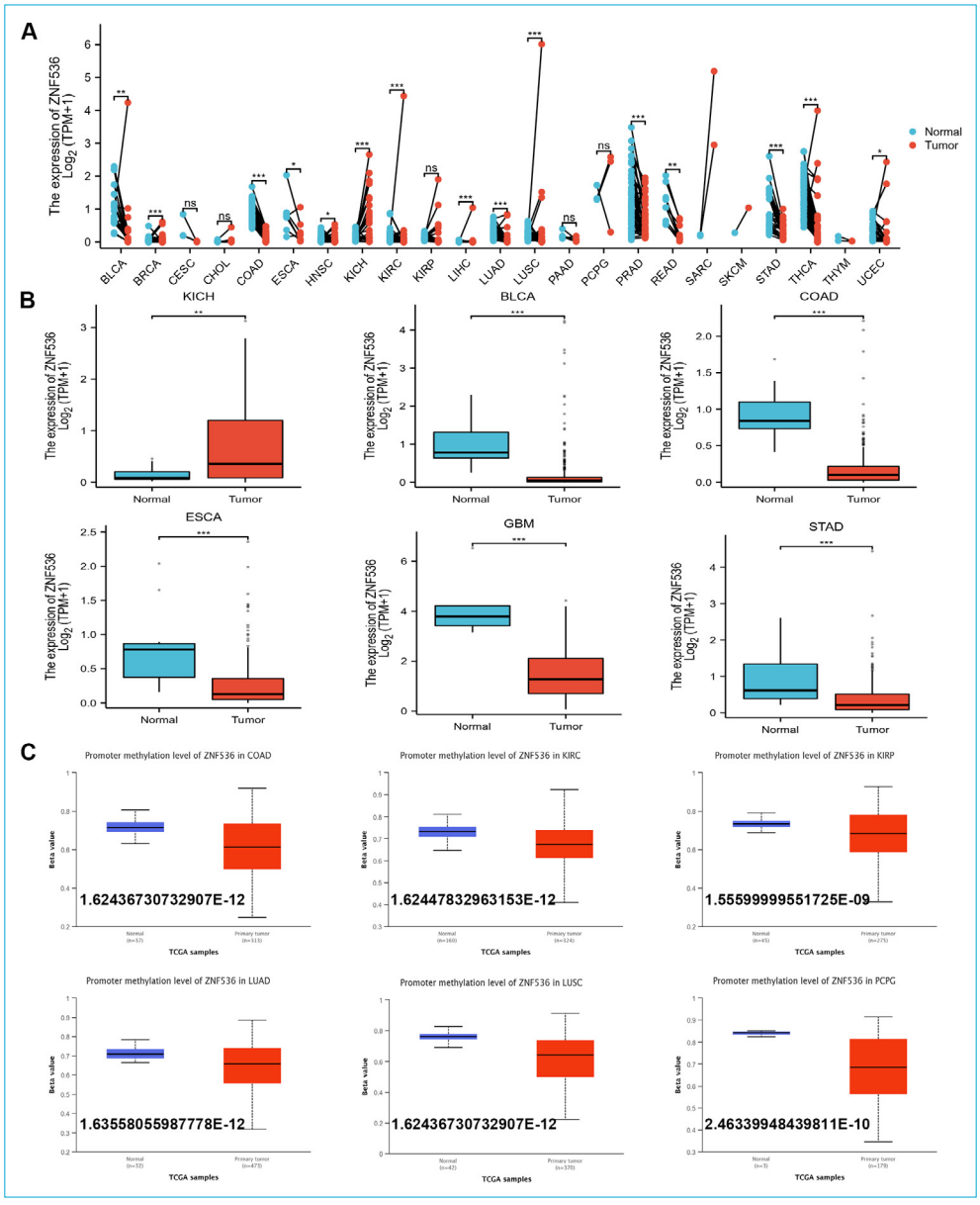

Supplementary Figure S1. Differential mRNA Expression and DNA Methylation of ZNF536 in Pan-Cancer. Differential expression analysis of ZNF536 mRNA based on TCGA and GTEx data in various cancers and their adjacent tissues **(a)**. ZNF536 mRNA expression was increased in KICH, but decreased in BLCA, COAD, ESCA, GBM, and STAD **(b)**. The DNA methylation was declined in COAD, KIRC, KIRP, LUAD, LUSC, and PCPG **(c)**. * represented p<0.05, ** represented p<0.01, and *** represented p<0.001, ns represented no statistical significance.

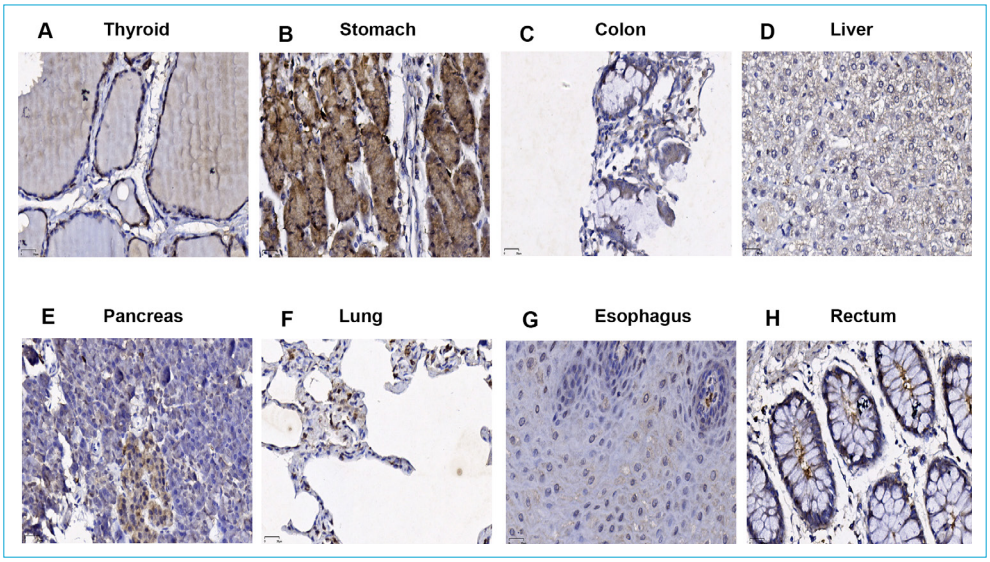

Supplementary Figure S2. Protein expression of ZNF536 in normal tissues of thyroid **(a)**, stomach **(b)**, colon **(c)**, liver **(d)**, pancreas **(e)**, lung **(f)**, esophagus **(g)** and rectum **(h)**. They were all originally magnified principal images (×200) with a scale bar of 30μm.

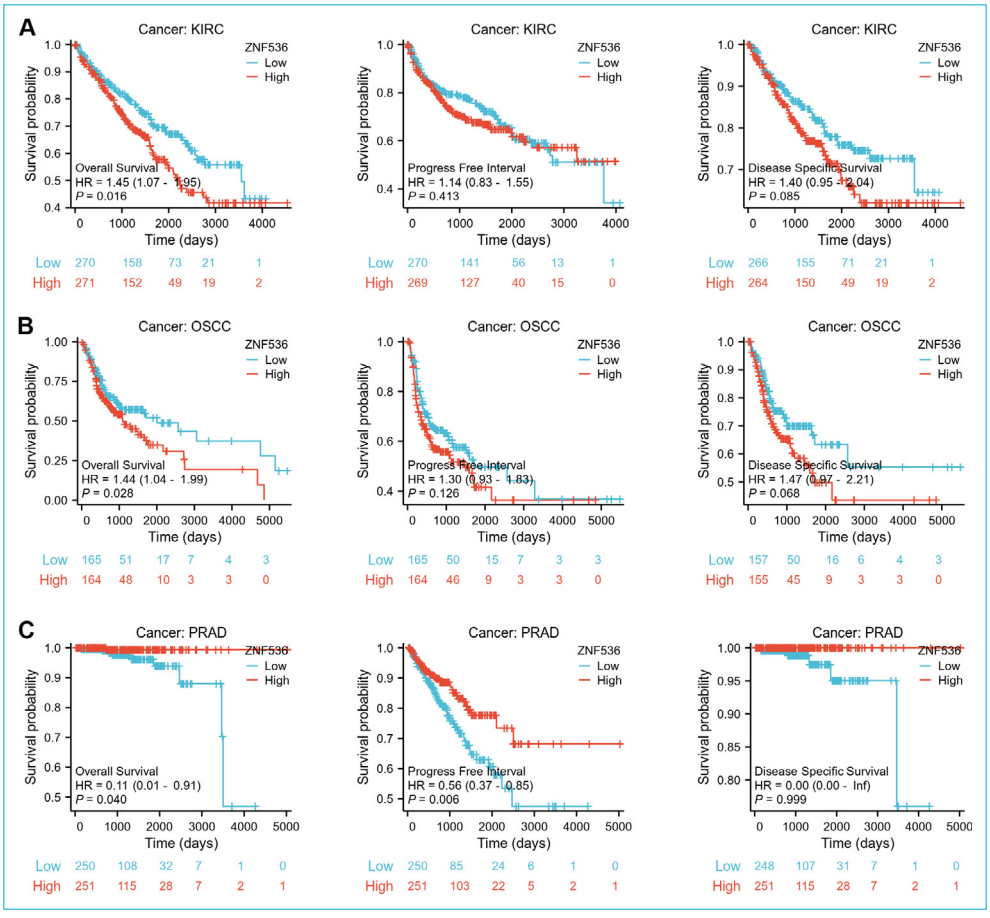

Supplementary Figure S3. Survival analysis of ZNF536 in pan-cancer. ZNF536 mRNA was negatively associated with OS in KIRC **(a)** and OSCC **(b)**. High expression of ZNF536 mRNA predicted favorable prognosis with lengthened OS and DSS in PRAD **(c)**.

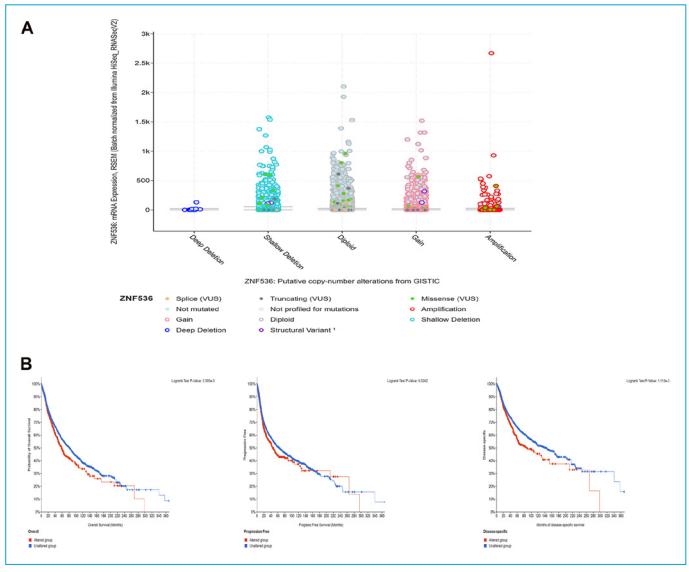

Supplementary Figure S4. Genomic alterations of ZNF536 in pan-cancer. The alteration types of ZNF536 in pan-cancer **(a)**. The survival of patients in ZNF536 altered group and unaltered group **(b)**.

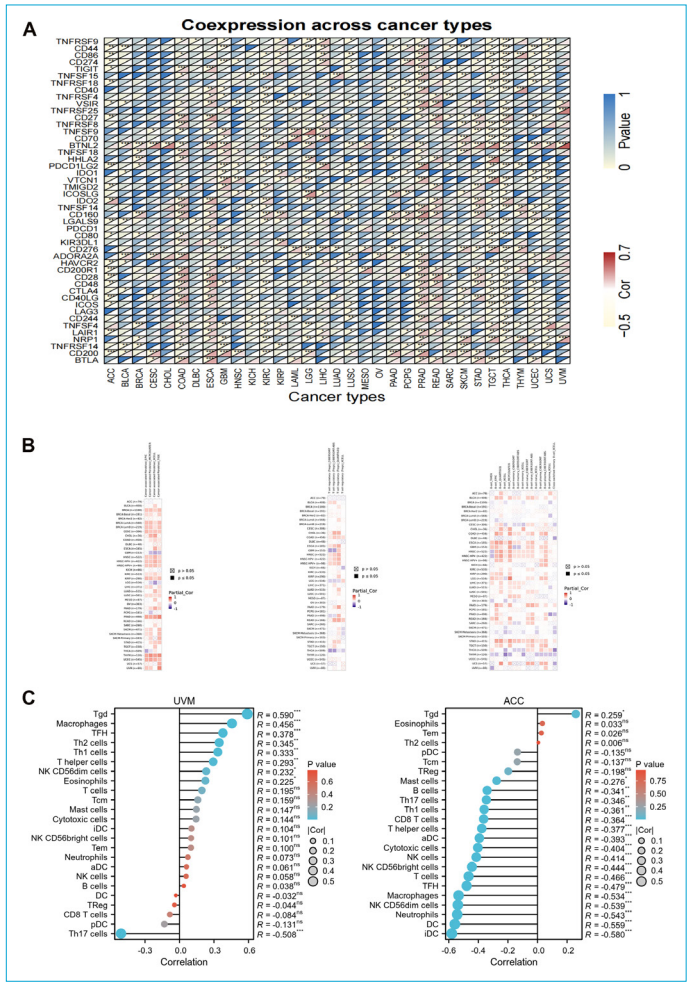

Supplementary Figure S5. Relationship between ZNF536 mRNA expression and tumor immune microenvironment. The co-expression heat map of ZNF536 and immune-related genes **(a)**. Relationship between ZNF536 mRNA expression and cancer associated fibroblasts, Tregs and B cells **(b)**. ZNF536 mRNA expression and most immune infiltrates was positively correlated in UVM but negatively correlated in ACC **(c)**. * represented p<0.05, ** represented p<0.01, and *** represented p<0.001, ns represented no statistical significance.

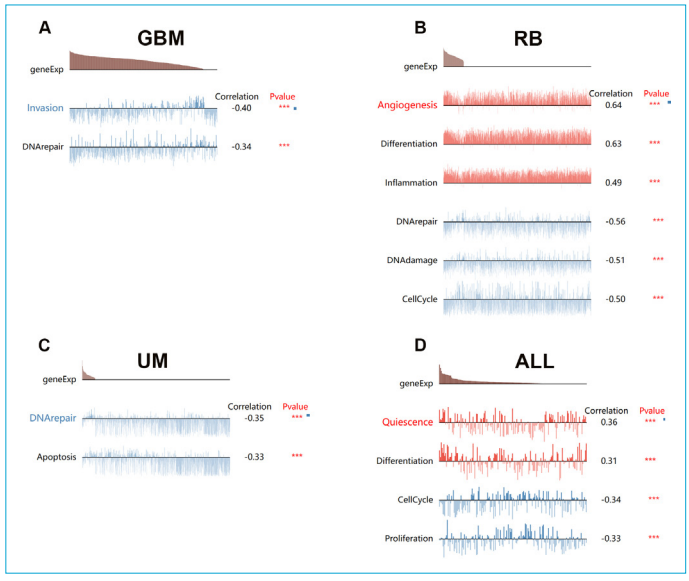

Supplementary Figure S6. The significant functional states in GBM **(a)**, RB **(b)**, UM **(c)**, and ALL **(d)**. *** represented p<0.001.

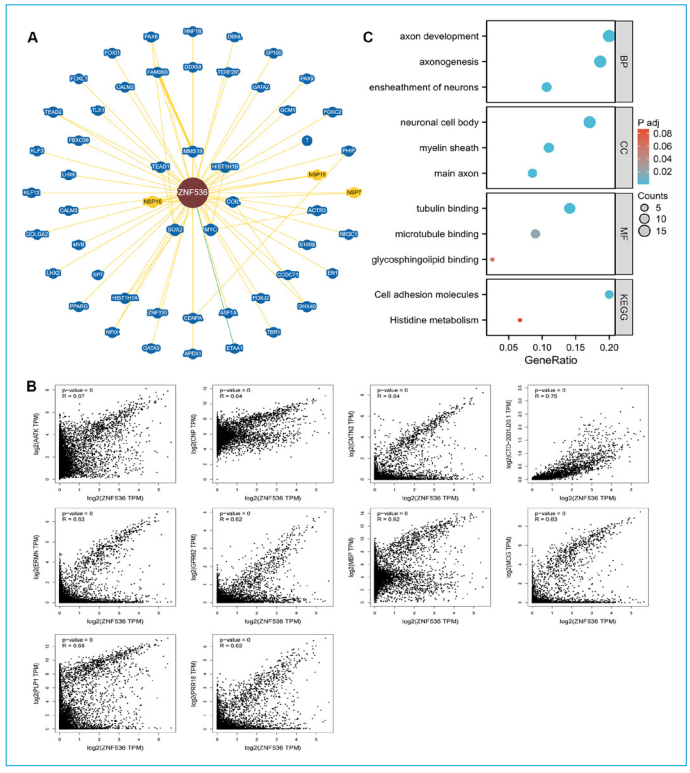

Supplementary Figure S7. Functional enrichment analysis of top 100 ZNF536 related genes. The network of ZNF536 and its related genes was displayed using BioGRID **(a)**. ZNF536 related genes, AATK, PLP1, CNTN2, CNP, MOG, ERMN, GPR62, PRR18, MBP, and MAG, were strongly associated with ZNF536 in the majority of cancer types **(b)**. GO and KEGG enrichment analysis of ZNF536 related genes **(c)**.